Journal of Medicinal Chemistry

Article

pubs.acs.org/jmc

Anti-Leukemic Activity of Ubiquinone-Based Compounds Targeting Trans-plasma Membrane Electron Transport

Carole Grasso,[†] Lesley Larsen,[§] Melanie McConnell,[†] Robin A. J. Smith,[§] and Michael V. Berridge*[,†]

[†]Malaghan Institute of Medical Research, P.O. Box 7060, Wellington, New Zealand

[§]Department of Chemistry, University of Otago, P.O. Box 56, Dunedin, New Zealand

Supporting Information

ABSTRACT: Trans-plasma membrane electron transport (tPMET) is a ubiquinone-dependent cell survival pathway for maintaining intracellular redox homeostasis in rapidly dividing cells. To target this pathway, fifteen ubiquinone-based compounds were designed and synthesized to position at the plasma membrane and disrupt tPMET. We established that quaternary ammonium salt moieties carrying highly hindered, positive electronic charges located to the plasma membrane. A ten-carbon chain linked to these moieties was effective at positioning the redox-active ubiquinone-like function within the lipid bilayer to disrupt tPMET in human leukemic cells (IC_{50} 9 ± 1 μM). TPMET inhibition alone was not sufficient to induce significant cell death, but positively charged compounds could also enter the cell and disrupt intracellular redox balance, distinct from their effects on mitochondrial electron transport. The synergistic effect of tPMET inhibition plus intracellular redox disruption gave strong antiproliferative activity (IC_{50} 2 ± 0.2 μM). Positively charged ubiquinone-based compounds inhibit human leukemic cell growth.

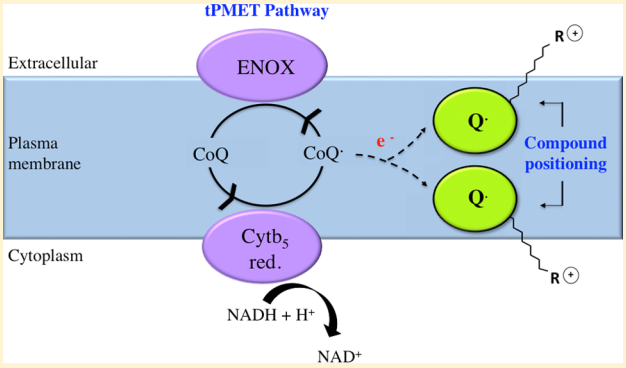

INTRODUCTION

The trans-plasma membrane electron transport (tPMET) complex is a simple redox-active ubiquinone system spanning the plasma membrane of all living cells. It is linked to a diverse range of biological functions including cell metabolism, defense, growth, and survival.[1−5] Electrons from intracellular reductants flow through enzyme-mediated tPMET pathways to reduce extracellular molecules,[2,6,7] allowing cells to respond to changes in their redox microenvironment and maintain intracellular NAD^+/NADH homeostasis.[8−10]

Cancer cells that use glycolytic metabolism to accommodate their metabolic demands even in the presence of oxygen[11−13] employ tPMET pathways in addition to lactate dehydrogenase to replenish NAD^+ pools.[14−17] A significant imbalance of the NAD^+/NADH ratio can create intracellular reductive stress resulting in cell death.[18−20] Due to the dependence of glycolytic cancer cells on tPMET for their survival, the pathway is a potential target for drug development.[21]

We have previously shown that the redox-active, anticancer drug, phenoxodiol, inhibits tPMET and is linked to antiproliferative activity in human leukemic HL60 cells.[22,23] Here, we report on the synthesis and structure−activity profile of a series of fifteen redox-active ubiquinone-based compounds designed to inhibit tPMET, and compare tPMET inhibition with antiproliferative activity against human leukemic HL60 cells. The compounds are composed of a redox-active dimethoxymethylquinone component, functionally related to ubiquinone, coupled by a 3, 5, or 10-carbon chain to a terminal moiety of varying polarity and/or electronic charge. These moieties are designed to position the active compound at the outer or inner leaflet of the plasma membrane, allowing the quinone component to locate within the lipid bilayer and disrupt redox cycling (Figure 1). Similar membrane positioning studies have been carried out with a series of MitoQ compounds where a 10-carbon (C10) chain was found to be most effective for antioxidant activity.[24]

We tested each compound for inhibition of tPMET activity and for antiproliferative activity in HL60 cells which have active mitochondrial and plasma membrane electron transport function, and HL60ρ^o mitochondrial gene-knockout cells that are defective in mitochondrial electron transport[25] but have elevated tPMET.[15] This allowed the effect of tPMET inhibition to be distinguished from inhibition of mitochondrial electron transport. We show that compounds in which a redox-active quinone is linked by a C10 chain to a quaternary ammonium salt with a highly hindered positive charge had the highest tPMET inhibitory activity and antiproliferative activity, independent of mitochondrial electron transport.

SYNTHESIS

Alcohols. The C3 (**1**) and C5 (**2**) alcohols were prepared as described by Hiroshi Morimoto[26] and our group, Asin-Cayuela et al.[27] The C10 compound idebenone (**3**) was obtained from commercial sources.

Sulfonic Acids. The sulfonic acids were prepared as outlined in Scheme 1. The key step in the synthesis was the use of the isobutyl

Received: July 12, 2012
Published: February 22, 2013

dx.doi.org/10.1021/jm301585z | J. Med. Chem. 2013, 56, 3168−3176

Scheme 1. Structures of 1−3 and 14[a]

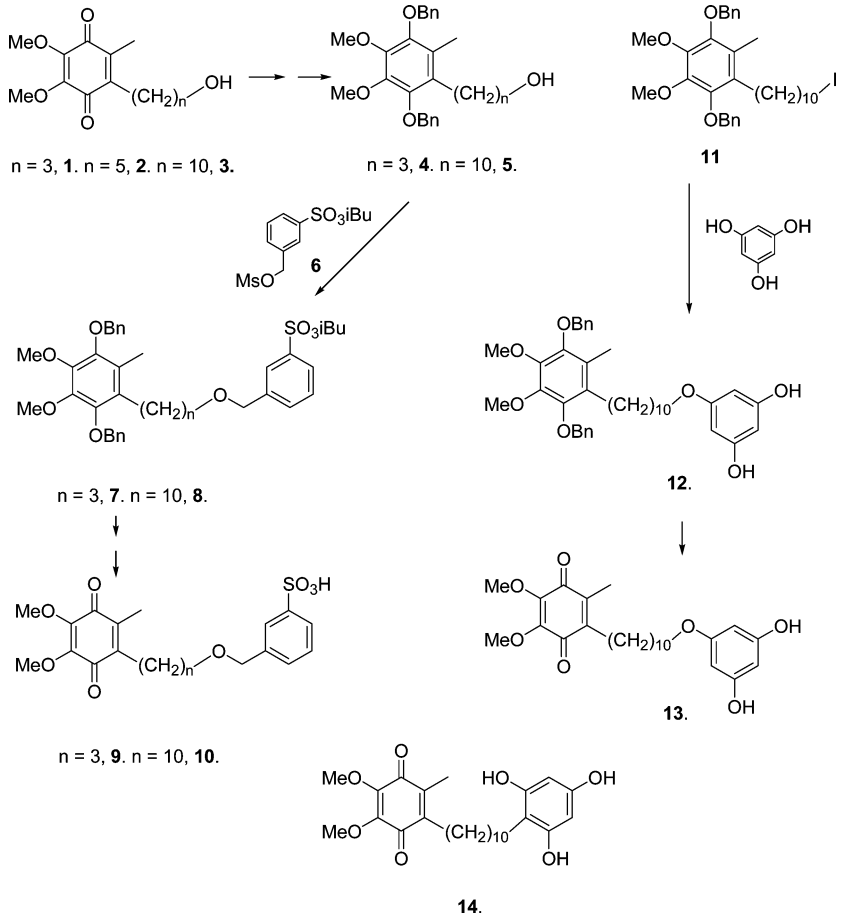

[a]Synthetic routes to **9**, **10**, and **13**.

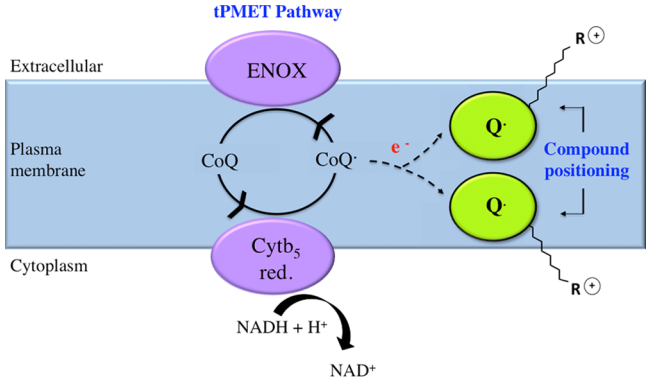

Figure 1. Model of enzyme-mediated tPMET pathway showing the positioning of ubiquinone-based compounds within the lipid bilayer to disrupt ubiquinone (CoQ) redox cycling via CoQ· during oxidation of intracellular NADH to NAD^+.

protecting group for aromatic sulfonic acids.[28] Reduction and O-benzylation[29] of **1** and **3** gave the alcohols (**4**, **5**), the anions of which were then reacted with mesylate **6** to produce the sulfonic esters (**7**, **8**). The sulfonate ester **6** was obtained from 3-(chlorosulfonyl)-benzoyl chloride by reaction with *iso*butanol, followed by reduction with RedAl then mesylation. Deprotection of **7** and **8** by hydrogenation, followed by oxidation in air and removal of the isobutyl group with sodium iodide, gave the required quinone sulfonic acids **9** and **10**.

Phloroglucinols. Alkylation of phloroglucinol with (**11**) using potassium carbonate in acetone gave the O-alkyated product (**12**) which was debenzylated by hydrogenation and oxidized in air to give **13**. The preparation of the corresponding C-alkylated compound (**14**) has been described by us previously.[29]

Amines and Quaternary Ammonium Salts. Nitrogen was introduced at the end of the alkyl chain by nucleophilic substitution of idebenone mesylate (**15**) with various amines in *tert*-butanol (Scheme 2). Reaction with imidazole, morpholine, or dibenzylamine gave the tertiary amines **16**, **17**, and **18**, respectively. Similar reaction of **15** with *N*-methylimidazole or *N*-methylmorpholine gave the quaternary salts **19**, **20**. Other quaternary salts, which could not be formed directly in this way, were obtained via alkylation of the appropriate amine; thus, benzyl bromide in dichloroethane was reacted with **16** to give **21** and reaction of **18** with excess methyl iodide led to the dibenzylmethylammonium salt **22**. The tribenzylammonium salt **23** was formed in low yield by the prolonged reaction of excess benzyl bromide and sodium iodide with **18** at 50 °C.

The synthetic yields, HPLC, ^1H NMR, and ESI-MS of unreported compounds are described in the Experimental Section and ^{13}C NMR data are presented in Table 2.

RESULTS AND DISCUSSION

Previous studies have shown that small, amphipathic, redox-active molecules have tPMET inhibitory activity (TIA) as well as antiproliferative activity (APA).[22,23] We therefore synthesized a

dx.doi.org/10.1021/jm301585z | J. Med. Chem. 2013, 56, 3168−3176

Scheme 2. Synthetic Routes to 16−23

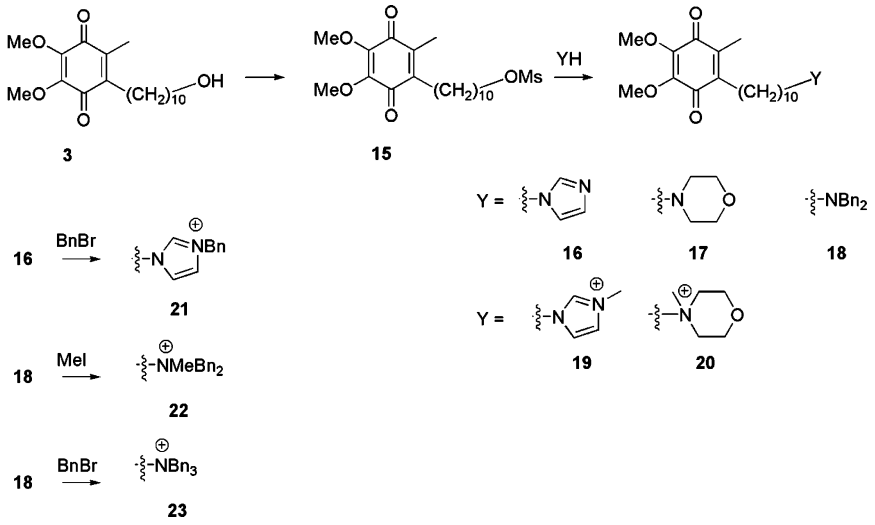

Table 1. In Vitro tPMET Inhibitory Activity and Antiproliferative Activity of Ubiquinone-Based Compounds

	tPMET inhibitory activity (TIA) IC_{50}[a] (μM)		antiproliferative activity (APA) IC_{50} (μM)	
compound	HL60	HL60ρ^o	HL60	HL60ρ^o
1	Inactive[b]	92 ± 22	13 ± 1	15 ± 5
2	Inactive	123 ± 53	13 ± 1	8 ± 3
3	77 ± 19	70 ± 4	36 ± 3	Inactive
9	Inactive	Inactive	Inactive	Inactive
10	81 ± 6	70 ± 5	143 ± 3	120 ± 5
13	6 ± 1	13 ± 2	16 ± 5	63 ± 35
14	21 ± 1	9 ± 1	Inactive	Inactive
16	14 ± 1	33 ± 9	3 ± 2	15 ± 13
17	33 ± 11	46 ± 8	3 ± 2	15 ± 13
18	Inactive	Inactive	33 ± 10	Inactive
19	23 ± 1	78 ± 8	35 ± 17	44 ± 10
20	122 ± 8	Inactive	1 ± 0.3	Inactive
21	9 ± 1	68 ± 6	2 ± 0.2	5 ± 2
22	10 ± 1	47 ± 4	3 ± 0.1	3 ± 0.4
23	14 ± 3	54 ± 12	2 ± 0.1	3 ± 1

[a]Values are means of dose−response experiments ± SEM (n = 2/3). IC_{50} = half maximal inhibitory concentration. [b]Inactive = IC_{50} > 200 μM.

series of 15 compounds composed of a redox-active quinone moiety, functionally related to ubiquinone, linked with either a 3, 5, or 10-carbon chain to a terminal moiety with varying polarity and/or electronic charge and investigated their TIA and APA. The compounds were designed to determine the optimum carbon chain length and charge required to position the quinone within the plasma membrane lipid bilayer and thereby disrupt tPMET activity (see Figure 1).

Compounds were tested directly for TIA by their ability to block reduction of the cell-impermeable tetrazolium salt WST-1[30,31] in real time following a 30 min preincubation. APA was measured by reduction of cell-permeable MTT after 48 h incubation with the compound. The IC_{50} for each compound was determined for TIA and APA. Data were compared between the human leukemic cell line HL60, which has active mitochondrial and plasma membrane electron transport function, and HL60ρ^o mitochondrial gene-knockout cells that are defective in mitochondrial electron transport[25] but have elevated tPMET.[15] This allowed the effect of tPMET inhibition to be distinguished from effects on mitochondrial electron transport (Table 1). The ability of key active compounds to induce apoptosis was also determined through cell cycle analysis at 24, 48, and 72 h.

Alcohols − 1, 2, and 3. Initial efforts focused on readily accessible, uncharged, polar C3, C5, and C10 quinone alcohols. Compounds **1** and **2** did not have TIA in HL60 cells but had the same moderate APA (13 ± 1 μM), suggesting these compounds did not position at the plasma membrane and disrupt tPMET, but entered the cell and were active intracellularly. There was, however, weak TIA in HL60ρ^o cells for **1** and **2** (92 ± 22 and 123 ± 53 μM, respectively), potentially due to HL60ρ^o cells having upregulated tPMET as a consequence of dysfunctional oxidative phosphorylation and increased cellular NADH.[15] APA activity of **1** and **2** with HL60ρ^o was similar to HL60 cells (15 ± 5 and 8 ± 3 μM) confirming that these compounds were not working primarily at the level of mitochondrial electron transport.

Compound **3** had weak TIA with HL60 and HL60ρ^o (77 ± 19 and 70 ± 4 μM), with moderate APA in HL60 cells (36 μM ± 3 μM) but no APA in HL60ρ^o, suggesting that, in addition to effects on tPMET, **3** was entering the cell and disrupting redox activity at the level of mitochondrial electron transport. These results support the view that inhibition of tPMET in HL60ρ^o cells is independent of mitochondrial electron transport. Cell cycle data for **3** showed cell cycle arrest in G1 in the surviving HL60 cells within 24 h with a 30 μM dose, but minimal cell cycle changes in HL60ρ^o cells (Figure 2).

Compounds with carbon chains longer than 10 were not considered given the synthetic chemical demands and our prior experience,[27] which indicated that incorporation of longer aliphatic chains resulted in very lipophilic compounds that did not interact effectively with cellular membranes. Well-known lipophilic biomolecules such as Coenzyme Q10 do not easily cross cell membranes but are synthesized and function within the hydrophobic core of membranes.

Overall, these results led to our designing compounds with a stronger negative charge and a restricted range of carbon-linker chains.

Sulfonic Acids − 9 and 10. Compounds **9** and **10** contain an arylsulfonic acid function which, at biological pH, would be completely deprotonated and thus embody a net negative charge. The short chain compound (**9**) resulted in inactive TIA and APA in both HL60 and HL60ρ^o cells, indicating the strong negative

dx.doi.org/10.1021/jm301585z | J. Med. Chem. 2013, 56, 3168−3176

Table 2. ^{13}C NMR Data for Compounds

	compound										
position	**9**[a]	**10**[a]	**13**[b]	**16**[b]	**17**[b]	**18**[b]	**19**[b]	**20**[b]	**21**[b]	**22**[b]	**23**[b]
1	186.3	186.3	184.8	184.7	184.7	184.6	184.6	184.6	184.6	184.5	184.6
2	146.1	146.1	144.3	144.3	144.3	143.9	144.2	144.2	144.2	144.2	144.3
3	146.1	146.1	144.2	144.3	144.2	143.1	144.2	144.2	144.2	144.1	144.2
4	185.8	185.9	184.4	184.2	184.1	184.1	184.1	184.1	184.1	184.0	184.1
5	144.1	144.4	143.2	143.0	143.0	140.1	143.0	143.0	142.9	142.8	142.9
6	140.7	140.3	138.9	138.7	138.6	138.6	138.7	138.7	138.6	138.6	138.7
OMe	61.9	61.9	61.2	61.1	61.1	61.1	61.1	61.1	61.1	61.0	61.1
OMe	61.9	61.9	61.2	61.1	61.1	61.1	61.1	61.1	61.1	61.0	61.1
ArMe	12.2	12.2	11.9	11.9	11.9	11.9	11.9	11.9	11.8	11.8	11.9
1′	24.6	27.4	25.8	26.4	26.3	26.4	26.1	21.8[c]	26.3	23.0	24.1
2′	29.9	27.6[c]	26.4[c]	26.5[c]	26.5[c]	27.0[c]	26.3[c]	26.0[c]	28.6	26.2	26.3
3′	71.3	30.0[c]	29.0[c]	28.7[c]	27.5[c]	27.2[c]	28.6[c]	26.3[c]	28.8[c]	28.4	26.8
4′		30.7[c]	29.0[c]	29.0[c]	28.7[c]	28.7[c]	28.8[c]	28.5[c]	29.1[c]	28.9	28.6
5′		30.8[c]	29.1[c]	29.3[c]	29.3[c]	29.3[c]	29.1[c]	29.0[c]	29.1[c]	29.1	28.8
6′		30.8[c]	29.1[c]	29.3[c]	29.4[c]	29.5[c]	29.2[c]	29.1[c]	29.1[c]	29.1	29.1
7′		30.9[c]	29.2[c]	29.3[c]	29.5[c]	29.6[c]	29.7[c]	29.1[c]	29.6[c]	29.1	29.1
8′		31.1[c]	29.7[c]	29.7[c]	29.5[c]	29.9[c]	30.2[c]	29.1[c]	26.1	29.2	29.1
9′		31.1[c]	28.6	31.1[c]	29.8[c]	29.8[c]	36.5[c]	29.6[c]	30.1	29.6	29.6
10′		72.0	68.0	47.0	59.8	58.2	50.0	59.9[c]	50.1	59.57	60.1
1″	73.5	73.6				53.4[c]			53.2	64.6	64.3
Ar1	140.5	140.9	161.3			126.6			133.0	127.0	128.0
Ar2	126.4	126.4	94.8			128.1			129.0	129.2	129.3
Ar3	146.1	146.1	157.6			128.7			129.3	133.1	133.2
Ar4	126.4	126.4	95.6			128.2			129.4	130.6	130.6
Ar5	129.7	129.7	157.6			128.7			129.3	133.1	133.2
Ar6	130.9	131.0	94.8			128.1			129.0	129.2	129.3
Im2				137.1			138.3		137.1		
Im4				129.4[c]			123.2[c]		121.8[c]		
Im5				118.7[c]			121.5[c]		121.8[c]		
NMe							39.6[c]	47.6[c]		46.4	
Morph2					53.8			60.7[c]			
Morph3					67.0			65.7[c]			

[a]CD_3OD solvent. [b]$CDCl_3$ solvent. [c]Denotes signals not formally assigned. Numbering systems as shown below.

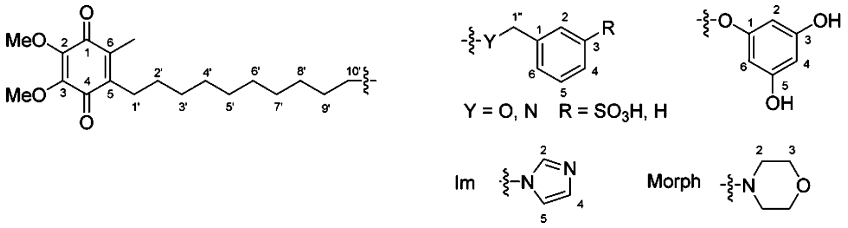

charge was potentially repelling the quinone function from the outer plasma membrane. This idea was supported by results with **10**, which showed weak TIA in HL60 and HL60ρ^o (81 ± 6 and 70 ± 5 μM) and weak APA (143 ± 3 and 120 ± 5 μM) indicating the longer alkyl chain was allowing the quinone to position within the lipid bilayer.

These results indicated the need for a moiety with reduced negative charge to prevent repulsion from the plasma membrane, and a sufficiently long carbon chain to allow the quinone to position within the lipid bilayer. Therefore, all further work concentrated on the longer C10 chain length exclusively.

Phloroglucinols − 13 and 14. Compound **13** is a C10 quinone linked to a phloroglucinol through oxygen with two residual free phenolic groups. Therefore at biological pH, **13** would be expected to have a small residual negative charge. Compound **13** had strong TIA in HL60 cells (6 ± 1 μM) and moderate APA (16 ± 5 μM), with cell death induced within 24 h with a 30 μM dose (data not shown). HL60ρ^o cells had moderately strong TIA (13 ± 2 μM), but weak APA (63 ± 35 μM), with cell death at 72 h. In contrast, **14**, a quinone linked through a C10 carbon to a phloroglucinol with three phenolic groups, had moderately strong TIA in HL60 (21 ± 1 μM) and HL60ρ^o (9 ± 1 μM) but no APA activity in either cell line. This suggests that **14** partitions at the plasma membrane and does not enter the cell, but tPMET inhibition alone is insufficient to induce cell death. Since **13** had similar TIA to **14** but also had APA, we suggest that **13** enters the cell where it has an intracellular target. Thus, a compound with synergistic effects on tPMET and on intracellular targets may have optimum activity against leukemic cells.

Amines −16, 17, and 18. Based on estimated pK_a values for **16**, **17** and **18**, **16** could be relatively protonated and therefore positively charged at biological pH compared to **17** and especially **18**. Results for **16** showed moderate TIA for HL60 (14 ± 1 μM) and HL60ρ^o (33 ± 9 μM), with strong APA in HL60 cells (3 ± 2 μM)

dx.doi.org/10.1021/jm301585z | J. Med. Chem. 2013, 56, 3168−3176

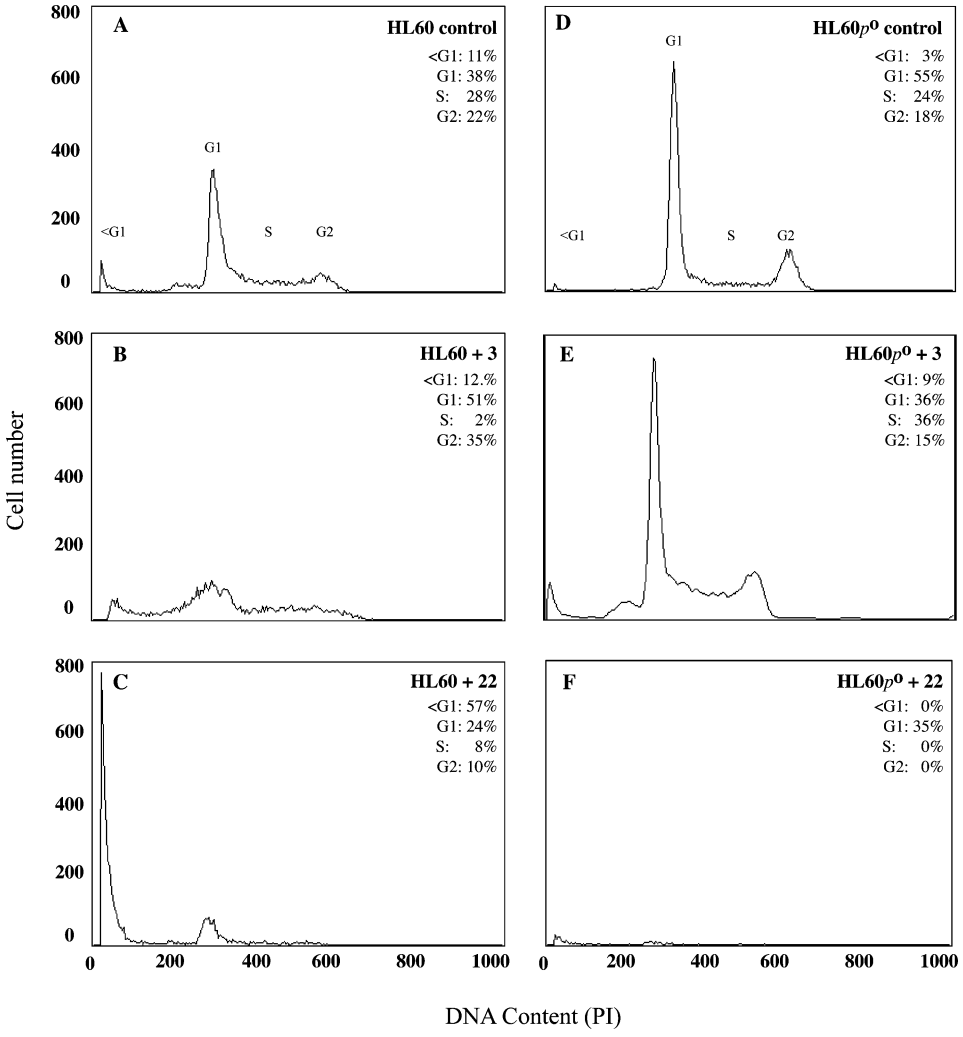

Figure 2. Effects of **3** and **22** on HL60 and HL60ρ^{o} on cell cycle arrest at 24 h time point. HL60 and HL60ρ^{o} cells were incubated with and without 30 μM **3** or **22** for 24 h, stained with propidium iodide (PI), and analyzed by flow cytometry to measure apoptosis by cell cycle arrest in G1 and accumulation of cells in <G1 in surviving cell populations. A. HL60. B. HL60 + 30 μM **3**. C. HL60 + 30 μM **22**. D. HL60ρ^{o}. E. HL60ρ^{o} + 30 μM **3**. F. HL60ρ^{o} + 30 μM **22**. Representative of 2 experiments.

and moderately strong activity in HL60ρ^{o} cells (15 ± 13 μM). Compound **17** showed a similar trend except that TIA for HL60 (33 ± 11 μM) was increased. In contrast, the most basic compound, **18**, had no TIA on HL60 or HL60ρ^{o} cells and only moderate APA effects on HL60 cells (33 ± 10 μM). Compound **18** appeared not to partition at the membrane, but was entering the cell and affecting the cell at the level of mitochondrial electron transport.

Results from **16** and **17** highlighted the potential synergy of positively charged compounds. Compounds with varying levels of delocalized positive charge were therefore synthesized and evaluated.

Quaternary Ammonium Salts − 19, 20, 21, 22, and 23. Compound **19** containing a dispersed, mildly hindered delocalized charge, had the least APA activity in this group of compounds, with only moderate (HL60) and weak (HL60ρ^{o}) TIA. The *N*-methylmorpholine salt **20**, whose positive charge is less distributed and moderately hindered had weak TIA for HL60 (122 ± 8 μM), but very strong APA (1 + 0.3 μM). Examination of **20** with HL60ρ^{o} cells showed no TIA or APA. These results give a strong indication that **20** is disrupting redox-sensitive mechanisms at the mitochondrial level. In contrast, the benzylimidazolium compound, **21**, with a hindered and delocalized positive charge, gave moderately strong TIA in HL60 cells (9 ± 1 μM) and weak TIA in HL60ρ^{o} cells (68 ± 6 μM), but very strong APA in both cell lines (2 and 5 ± 2 μM). These promising results led to the synthesis of **22** and **23**, highly hindered, positively charged compounds that could potentially inhibit tPMET and disrupt intracellular redox systems thereby maximizing inhibition of cell proliferation.

The dibenzylmethylammonium salt, **22**, and tribenzylammonium salt, **23**, both gave very strong APA in both cell lines (2−3 μM), with cell death induced within 24 h with a 30 μM dose (see Figure 2). However, TIA was moderate in HL60 cells (10 ± 1 and 14 ± 3 μM) and weak in HL60ρ^{o} cells (47 ± 4 and 54 ± 12 μM). These results again strongly suggest that these compounds interact intracellularly, but not at the level of mitochondrial electron transport.

■ CONCLUSION

Ubiquinone-like functions linked by a C10 carbon chain to quaternary ammonium salts with a highly hindered positive electronic charge had both the greatest inhibition of tPMET and highest antiproliferative activity in vitro, independent of mitochondrial electron transport. Our data suggest that these compounds

dx.doi.org/10.1021/jm301585z | J. Med. Chem. 2013, 56, 3168−3176

partition at the plasma membrane to inhibit tPMET activity but this inhibition alone is not sufficient to induce cell death. These positively charged compounds also enter the cell to disrupt non-mitochondrial redox-sensitive mechanisms and it is this synergistic effect that creates strong antiproliferative effects in human leukemic cells.

We conclude that C10 ubiquinone-based compounds with highly hindered, positively charged moieties are promising candidates for further development as anticancer drugs.

EXPERIMENTAL SECTION

General Chemistry Methods. Merck silica gel 60, 200−400 mesh, 40−63 μm, was used for silica gel chromatography. TLC was carried out using Merck Silica gel 60 F254, first visualized with a UV lamp, and then by dipping in a vanillin solution (1% vanillin, 1% H_2SO_4 in EtOH) and heating. High resolution mass spectrometry (HRMS) was recorded using a Bruker microTOF electrospray mass spectrometer. UV spectra were recorded in methanol using a Jasco V-550. IR spectra were recorded on a Bruker Optics Alpha FT-IR spectrometer (with a diamond Attenuated Total Reflectance (ATR) top plate). NMR spectra, at 25 °C, were recorded at 500 or 300 MHz for ^{1}H and 125 or 75 MHz for ^{13}C on Varian INOVA-500 or VXR-300 spectrometers. Chemical shifts are given in ppm on the δ scale referenced to the solvent peaks C**H**Cl_3 at 7.26 and **C**DCl_3 at 77.0; or $(CH_3)_2CO$ at 2.15 and $(CD_3)_2CO$ at 30.5; or C**H**$_3$OD at 3.3 and **C**D_3OD at 49.0; or $(CH_3)_2SO$ at 2.62 and $(CD_3)_2SO$ at 39.6. ^{13}C NMR data are presented in Table 2. All tested compounds had a purity of ≥95% shown by HPLC.

HPLC Methods. *Method A.* HPLC analysis was carried out using an Agilent HP1100 at 25 °C on a C18 column (Phenomenex Luna ODS(3) 5 μm 100 A 150 × 3 mm) with a 2 × 4 mm C18 guard column. Peaks were detected at 210 and 254 nm and UV spectra recorded from 190 to 600 nm. The mobile phase was acetonitrile in water, both with 0.1% formic acid: t_0 = 10%, $t_{12.5}$ = 100%, t_{15} = 100%, t_{16} = 10%, t_{20} = 10%. The flow rate was 0.5 mL/min, with an injection volume of 5 μL.

Method B. HPLC analysis was carried out using an Agilent HP1100 at 25 °C on a C8 column (Agilent Zorbax Eclipse XDB-C8 5 μm 100 A 150 × 4.6 mm) with a 2 × 4 mm C8 guard column. Peaks were detected at 210 and 254 nm and UV spectra recorded from 190 to 600 nm. The mobile phase was methanol in water, both with 0.1% trifluoroacetic acid: t_0 = 10%, $t_{12.5}$ = 100%, t_{15} = 100%, t_{16} = 10%, t_{20} = 10%. The flow rate was 0.5 mL/min, with an injection volume of 5 μL.

Procedures for the Synthesis of Compounds. *Isobutyl 3-[3-(2,5-Bis(benzyloxy)-3,4-dimethoxy-6-methylphenyl)-propyloxymethylene]benzenesulfonate (**7**).* To a stirred solution of 3,4-dimethoxy-6-methyl-2,5-bis(phenylmethoxy)-benzenepropanol (**4**) (0.13 g, 0.31 mmol) in dry dimethylformamide (0.5 mL) at RT was added sodium hydride (20 mg, 60% w/w, 0.47 mmol) and the mixture stirred for 0.5 h. Isobutyl 3-(mesyloxymethyl)benzenesulfonate (**7**) (0.10 g, 0.31 mmol) was added and stirring continued for 12 h. The mixture was added to ice/water then extracted into dichloromethane (DCM). Purification by column chromatography over silica gel eluting with DCM/ethyl acetate gave **7** (115 mg, 57%) as a colorless oil. ^{1}H NMR ($CDCl_3$) δ: 7.85 (1H, s), 7.81 (1H, d, J = 8 Hz), 7.59 (1H, d, J = 8 Hz), 7.29−7.53 (11H, m), 5.00 (2H, s), 4.96 (2H, s), 4.52 (2H, s), 3.95 (3H, s), 3.94 (3H, s), 3.80 (2H, d, J = 7 Hz), 3.50 (2H, t, J = 7 Hz), 2.70 (2H, m), 2.16 (3H, s), 1.94 (1H, m), 1.75 (2H, m), and 0.88 (6H, d, J = 7 Hz); HRMS (+ve ESI) calc for $C_{37}H_{44}NaO_8S$ 671.2649 m/z [MNa^+], found 671.2644 m/z.

*Isobutyl 3-[10-(2,5-Bis(benzyloxy)-3,4-dimethoxy-6-methylphenyl)decyloxymethylene]benzenesulfonate (**8**).* Similarly, treatment of 3,4-dimethoxy-6-methyl-2,5-bis(phenylmethoxy)-benzenedecanol (**5**)[29] (0.10 g, 0.31 mmol) with isobutyl 3-(mesyloxymethyl)benzenesulfonate (**7**) (0.16 g, 0.31 mmol) gave **8** as a colorless oil (70 mg, 30%). ^{1}H NMR ($CDCl_3$) δ: 7.88 (1H, bs), 7.81 (1H, bd, J = 8 Hz), 7.62 (1H, bd, J = 8 Hz), 7.52 (1H, t, J = 8 Hz), 7.49 (4H, bd), 7.39 (4H, bt), 7.34 (2H, bt), 5.00 (2H, s), 4.95 (2H, s), 4.56 (2H, s), 3.94 (3H, s), 3.93 (3H, s), 3.81 (2H, d, J = 7 Hz), 3.50 (2H, t, J = 7 Hz), 2.57 (2H, bt, J = 7 Hz), 2.15 (3H, s), 1.95 (1H, m), 1.63 (2H, m), 1.24−1.44 (14H, m), and 0.89 (6H, d, J = 7 Hz). HRMS (+ve ESI) calc for $C_{44}H_{58}NaO_8S$ 769.3745 m/z [MNa^+], found 769.3791 m/z.

*3-[3-(2,5-Dioxo-3,4-dimethoxy-6-methylphenyl)-propyloxymethylene]benzenesulfonic Acid (**9**).* A solution of isobutyl 3-[3-(2,5-bis(benzyloxy)-3,4-dimethoxy-6-methylphenyl)propyloxymethylene]benzenesulfonate (**7**) (0.20 g, 0.31 mmol) in methanol (20 mL) in the presence of Pd/C (5 mg, 5%) was stirred under hydrogen for 60 min when TLC showed that all the starting material had been consumed. The mixture was then stirred in air overnight, filtered through Celite, and the solvents removed in vacuo to give a yellow gum. Purification by column chromatography over silica gel eluting with DCM/ethyl acetate gave isobutyl 3-[3-(2,5-dioxo-3,4-dimethoxy-6-methylphenyl)propyloxymethylene]benzenesulfonate as a yellow gum (90 mg, 62%). HPLC: 13.50 min (method A), 14.32 min (method B). ^{1}H NMR ($CDCl_3$) δ: 7.97 (1H, bs), 7.82 (1H, bd, J = 8 Hz), 7.61 (1H, bd, J = 8 Hz), 7.53 (1H, t, J = 8 Hz), 4.55 (2H, s) 3.97 (6H, s), 3.82 (2H, d, J = 7 Hz), 3.53 (2H, t, J = 7 Hz), 2.59 (2H, t, J = 7 Hz), 2.04 (3H, s), 1.95 (1H, m), 1.76 (2H, m), and 0.89 (6H, d, J = 7 Hz). HRMS (+ve ESI) calc for $C_{23}H_{30}NaO_8S$ 489.1554 m/z [MNa^+], found 489.1567 m/z.

A stirred solution of isobutyl 3-[3-(2,5-dioxo-3,4-dimethoxy-6-methylphenyl)propyloxymethyl]benzenesulfonate (90 mg) in dry acetonitrile (10 mL) with sodium iodide (90 mg) was heated to reflux for 3 h when TLC analysis showed all the starting material had been consumed. Evaporation of the solvent in vacuo and purification by column chromatography over silica gel eluting with chloroform/methanol 0−20% gave quinone **9** as an orange solid (40 mg, 51%). This was dissolved in water and freeze−dried to give a fluffy orange solid. HPLC: 9.66 min (method A). ^{1}H NMR (CD_3OD) δ: 7.84 (1H, s), 7.78 (1H, d, J = 7 Hz), 7.44 (2H, m), 4.52 (2H, s) 3.93 (6H, s), 3.55 (2H, t, J = 7 Hz), 2.61 (2H, t, J = 7 Hz), 2.03 (3H, s), and 1.76 (2H, m). HRMS (−ve ESI) calc for $C_{19}H_{21}O_8S$ 409.0963 m/z [M-H$^-$], found 409.0987 m/z.

*3-[10-(2,5-Dioxo-3,4-dimethoxy-6-methylphenyl)-decyloxymethylene]benzenesulfonic Acid (**10**).* Similarly, treatment of **8** (0.20 g, 0.27 mmol) gave isobutyl 3-[10-(2,5-dioxo-3,4-dimethoxy-6-methylphenyl)decyloxymethylene]-benzenesulfonate (0.11 g, 73%) as an orange solid. HPLC: 16.40 min (Method A). ^{1}H NMR ($CDCl_3$) δ: 7.87 (1H, bs), 7.81 (1H, bd, J = 8 Hz), 7.63 (1H, bd, J = 8 Hz), 7.53 (1H, t, J = 8 Hz), 4.56 (2H, s), 3.99 (3H, s), 3.98 (3H, s), 3.81 (2H, d, J = 7 Hz), 3.50 (2H, t, J = 7 Hz), 2.44 (2H, bt, J = 7 Hz), 2.01 (3H, s), 1.95 (1H, m), 1.63 (2H, m), 1.24−1.44 (14H, m), and 0.89 (6H, d, J = 7 Hz). HRMS (+ve ESI) calc for $C_{30}H_{44}NaO_8S$ 587.2649 m/z [MNa^+], found 587.2665 m/z.

Similarly, isobutyl 3-[10-(2,5-dioxo-3,4-dimethoxy-6-methylphenyl)decyloxymethylene]benzenesulfonate (25 mg, 0.044 mmol) gave sulfonic acid **10** as an orange solid (11 mg, 47%). HPLC: 13.56 min (Method A). ^{1}H NMR (CD_3OD) δ: 7.83 (1H, bs), 7.75 (1H, bd, J = 8 Hz), 7.43 (1H, bd, J = 8 Hz), 7.40 (1H, t, J = 8 Hz), 4.52 (2H, s), 3.94 (6H, s), 3.48 (2H, t, J = 6 Hz),

dx.doi.org/10.1021/jm301585z | J. Med. Chem. 2013, 56, 3168−3176

2.45 (2H, m), 1.98 (3H, s), 1.59 (2H, m), and 1.28−1.40 (14H, m). HRMS (−ve ESI) calc for $C_{26}H_{35}O_8S$ 507.2058 m/z [M-H$^-$], found 507.2077 m/z.

*5-[10-(2,5-Bis(benzyloxy)-3,4-dimethoxy-6-methylphenyl)-decyloxy]benzene-1,3-diol (**12**).* A solution of phloroglucinol (0.30 g, 2.4 mmol) and 1-(10-iododecyl)-3,4-dimethoxy-6-methyl-2,5-bis(phenylmethoxy)benzene (**11**)[28] (0.20 g, 0.32 mmol) in acetone (5 mL) containing potassium carbonate (0.30 g, 2.2 mmol) was refluxed for 6 h. Treatment with 3 M HCl until acidic, extraction into ethyl acetate, drying, and evaporation in vacuo gave a brown gum. Purification by column chromatography over silica gel eluting with methanol in chloroform gave **12** (65 mg, 33%) as a pale yellow gum. HPLC 16.70 min (Method A), 16.82 min (Method B). ^{1}H NMR ($CDCl_3$) δ: 7.48 (4H, m), 7.38 (4H, m), 7.34 (2H, m), 5.96 (2H, s), 5.89 (1H, bs), 5.00 (2H, s), 4.95 (2H, s), 3.94 (3H, s), 3.93 (3H, s), 3.84 (2H, t, J = 7 Hz), 2.56 (2H, bt, J = 7 Hz), 2.14 (3H, s), 1.71 (2H, quin, J = 7 Hz), 1.39 (4H, m), and 1.24−1.31 (10H, m). ^{13}C NMR ($CDCl_3$) δ: 161.2, 157.5 (2C), 146.7, 146.6, 144.8, 144.8, 138.0, 137.7, 130.8, 128.4 (2C), 128.2 (2C), 127.9 (2C), 127.9 (2C), 127.8 (2C), 125.5, 95.5, 94.8 (2C), 75.4, 75.1, 69.0, 61.3, 61.3, 30.1, 30.0, 29.4, 29.3 (5), 29.3, 29.2, 29.1, 27.2, 25.9, and 12.0. HRMS (+ve ESI) calc for $C_{39}H_{48}NaO_7$ 651.3292 m/z [MNa$^+$], found 651.3278 m/z.

*5-[10-(2,5-Dioxo-3,4-dimethoxy-6-methylphenyl)-decyloxy]benzene-1,3-diol (**13**).* A solution of compound **12** (56 mg, 0.09 mmol) in methanol (10 mL) containing Pd/C (10%, 4 mg) was stirred under an atmosphere of hydrogen for 3 h when TLC showed that all the starting material had been consumed. The mixture was then stirred in air overnight, filtered through Celite, and the solvents removed in vacuo to give **13** (38 mg, 96%) as a yellow gum. HPLC: 13.34 min (Method A), 15.00 min (Method B). ^{1}H NMR ($CDCl_3$) δ: 5.99 (2H, s), 5.97 (1H, bs), 5.53 (2H, bs), 3.98 (3H, s), 3.97 (3H, s), 3.86 (2H, t, J = 7 Hz), 2.44 (2H, dd, J = 6 Hz, 7 Hz), 2.00 (3H, s), 1.71 (2H, quin, J = 7 Hz), 1.38 (4H, m), and 1.24−1.31 (10H, m). HRMS (+ve ESI) calc for $C_{25}H_{34}NaO_7$ 469.2197 m/z [MNa$^+$], found 469.2198 m/z. IR: υ_{max} 3405, 2928, 2855, 1644, 1610, 1468, and 1266 cm^{-1}. UV: λ_{max} (log ε) 411 (2.52) and 277 (4.15) nm.

*2-(10-Imidaz-1-yl)decyl-5,6-dimethoxy-3-methylcyclohexa-2,5-diene-1,4-dione (**16**).* A solution of the quinone mesylate **15** (100 mg, 0.24 mmol) and imidazole (200 mg, 0.73 mmol) in *tert*-butanol (10 mL) was refluxed for 2 h. The solvent was removed in vacuo, then the crude product purified by column chromatography over silica gel when 5% methanol in chloroform eluted **16** as a yellow solid (67 mg, 72%). HPLC: 9.38 min (Method A), 12.61 min (Method B). Found: C, 67.84; H, 8.43; and N, 7.09. $C_{22}H_{32}N_2O_4$ requires: C, 68.01; H, 8.30; and N, 7.21. ^{1}H NMR ($CDCl_3$) δ: 7.44 (1H, bs), 7.04 (1H, bs), 6.89 (1H, bs), 3.97 (6H, s), 3.90 (2H, t, J = 7 Hz), 2.43 (2H, t, J = 7 Hz), 1.99 (3H, s), 1.75 (4H, m), and 1.26 (16H, m). HRMS (+ve ESI) calc for $C_{22}H_{32}N_2O_4$ 389.2435 m/z [MH$^+$], found 389.2417 m/z. IR: υ_{max} 2928, 2855, 1651, 1610, 1456, 1267 cm^{-1}. UV: λ_{max} (log ε) 411 (2.49) and 278 (4.14) nm.

*2,3-Dimethoxy-5-methyl-6-[10(4-morpholinyl)decyl]-2,5-cyclohexadiene-1,4-dione (**17**).*[25] Similarly, quinone mesylate **15** (110 mg, 0.264 mmol) and morpholine (100 mg, 1.1 mmol) in *tert*-butanol (10 mL) gave **17** as a yellow gum (62 mg, 59%). HPLC: 9.03 min (Method A), 12.43 min (Method B). ^{1}H NMR ($CDCl_3$) δ: 3.96 (6H, s), 3.68 (4H, t, J = 8 Hz), 2.42 (6H, m), 2.28 (2H, dd, J = 7,8 Hz), 1.98 (3H, s), 1.45 (2H, m), 1.35 (2H, m), and 1.24−1.30 (12H, m). HRMS (+ve ESI) calc for $C_{23}H_{38}NO_5$ 408.2744 m/z [MH$^+$], found 408.2761m/z. IR υ_{max} 3439, 2929, 2853, 1647, 1610, 1461, 1272 cm^{-1}. UV λ_{max} (log ε) 421 (2.11) and 281 (3.68) nm.

*2-[10-(Dibenzylamino)decyl]-5,6-dimethoxy-3-methyl-2,5-cyclohexadiene-1,4-dione (**18**).* Similarly quinine mesylate **15** (100 mg, 0.24 mmol) and dibenzylamine (200 mg, 0.96 mmol) gave **18** as a yellow gum (82 mg, 66%). HPLC: 11.07 min (Method A), 13.92 min (Method B). Found: C, 75.15; H, 8.68; N, 2.54. $C_{33}H_{43}NO_4$. 1/2H_2O requires: C, 75.25; H, 8.42; N, 2.66. ^{1}H NMR ($CDCl_3$) δ: 7.18−7.38 (10H, m), 3.99 (6H, s), 3.54 (4H, s), 2.43 (2H, m), 2.38 (2H, t, J = 8 Hz), 2.01 (3H, s), 1.49 (2H, m), and 1.10−1.40 (14H, m). HRMS (+ve ESI) calc for $C_{33}H_{44}NO_4$ 518.3265 m/z [MH$^+$], found 518.3268 m/z. IR υ_{max} 2927, 2854, 1650, 1611, 1494, 1453, and 1266 cm^{-1}. UV λ_{max} (log ε) 387 (2.55) and 279 (4.01) nm.

*3-[10(4,5-Dimethoxy-2-methyl-3,6-dioxo-cyclohexa-1,4-dienyl)decyl]-1-methyl-3H-imidazol-1-ium Mesylate (**19**).* Similarly, quinone mesylate **15** (110 mg, 0.26 mmol) and *N*-methylimidazole (200 mg, 24 mmol) in *tert*-butanol (10 mL) gave **19** as an orange gum (56 mg, 54%). HPLC 9.47 min (Method A), 12.54 min (Method B). ^{1}H NMR ($CDCl_3$) δ: 9.95 (1H, bs), 7.36 (1H, bs), 7.26 (1H, s), 4.24 (2H, t, J = 8 Hz), 4.04 (3H, s), 3.96 (6H, s), 2.75 (3H, s), 2.41 (2H, m), 1.98 (3H, s), 1.86 (2H, m), and 1.20−1.35 (14H, m). HRMS (+ve ESI) calc for $C_{23}H_{35}N_2O_4$ 403.2591 m/z [M$^+$], found 403.2584 m/z. IR υ_{max} 3440, 2929, 2853, 1647, 1610, 1575, 1460, 1273, 1193 cm^{-1}. UV λ_{max} (log ε) 420 (2.06) and 278 (3.86) nm.

*4-[10(4,5-Dimethoxy-2-methyl-3,6-dioxo-cyclohexa-1,4-dienyl)decyl]-4-methylmorpholin-4-ium Mesylate (**20**).* Similarly, quinone mesylate **15** (110 mg, 0.24 mmol) and *N*-methylmorpholine (100 mg, 0.99 mmol) in *tert*-butanol (10 mL) gave **20** as a yellow gum (42 mg, 42%). HPLC: 8.96 min (Method A), 12.15 min (Method B). ^{1}H NMR ($CDCl_3$) δ: 3.95−4.20 (4H, m), 3.96 (6H, s), 3.55−3.90 (6H, m), 3.52 (3H, s), 2.41 (2H, m), 1.98 (3H, s), 1.79 (2H, m), and 1.20−1.40 (14H, m). HRMS (+ve ESI) calc for $C_{24}H_{40}NO_5$ 422.2901 m/z [M$^+$], found 422.2897 m/z. IR υ_{max} 3439, 2926, 2854, 1647, 1610, 1456, 1267 cm^{-1}. UV λ_{max} (log ε) 387 (2.67) and 278 (4.06) nm.

*3-[10(4,5-Dimethoxy-2-methyl-3,6-dioxo-cyclohexa-1,4-dienyl)decyl]-1-benzyl-3H-imidazol-1-ium Mesylate (**21**).* A solution of the imidazole quinone **16** (70 mg, 0.18 mmol) and benzyl bromide (100 mg, 0.88 mmol) in dichloroethane (7 mL) was refluxed for 2 h. The solvent was removed in vacuo, then the crude product purified by column chromatography over silica gel when 5% methanol in chloroform eluted **21** as a yellow gum (45 mg, 52%). HPLC: 10.54 min (Method A), 13.29 min (Method B). ^{1}H NMR ($CDCl_3$) δ: 10.60 (1H, s), 7.46 (2H, m), 7.33 (3H, m), 7.31 (2H, s), 5.58 (2H, s), 4.25 (2H, t, J = 7.5 Hz), 3.94 (6H, s), 2.39 (2H, t, J = 7 Hz), 1.96 (3H, s), 1.86 (2H, m), 1.32 (2H, m), 1.28 (2H, m), and 1.25 (10H, m). HRMS (+ve ESI) calc for $C_{29}H_{39}N_2O_4$ 479.2904 m/z [M$^+$], found 479.2892 m/z. IR υ_{max} 3418, 2927, 2855, 1650, 1610, 1562, 1456, and 1266 cm^{-1}. UV λ_{max} (log ε) 416 (2.39) and 278 (4.05) nm.

*Dibenzyl[10(4,5-dimethoxy-2-methyl-3,6-dioxo-cyclohexa-1,4-dienyl)decyl]methylammonium Mesylate (**22**).* A solution of the dibenzylaminoquinone **18** (100 mg, 0.19 mmol) in methyl iodide (5 mL) was stood for 18 h. The solvent was removed in vacuo, then the crude product purified by column chromatography over silica gel when 5% methanol in chloroform eluted **22** as a yellow gum (82 mg, 64%). HPLC: 11.15 min (Method A), 13.71 min (Method B). ^{1}H NMR ($CDCl_3$) δ: 7.61 (4H, d, J = 8 Hz), 7.40 (6H, m), 4.99 (4H, s), 3.94 (6H, s), 3.22 (2H, m), 3.07 (3H, s), 2.40 (2H, t, J = 7 Hz), 1.97 (3H, s), 1.94 (2H, m), and 1.10−1.40 (14H, m). HRMS (+ve ESI) calc

for $C_{34}H_{46}NO_4$ 532.3421 m/z [M^+], found 532.3415 m/z. IR υ_{max} 2927, 2854, 1651, 1611, 1456, and 1267 cm^{-1}. UV λ_{max} (log ε) 387 (2.31) and 278 (3.95) nm.

*Tribenzyl[10-(4,5-dimethoxy-2-methyl-3,6-dioxo-cyclohexa-1,4-dienyl)decyl]ammonium Mesylate (**23**).* A solution of the quinone **18** (50 mg, 0.096 mmol) and benzyl bromide (70 mg, 0.40 mmol) with sodium iodide (70 mg) was heated at 50 °C for 96 h. The solvent was removed in vacuo, then the crude product purified by column chromatography over silica gel when 10% methanol in chloroform eluted **23** as an orange gum (12 mg, 18%). HPLC: 12.01 min (Method A), 14.32 min (Method B). ^{1}H NMR ($CDCl_3$) δ: 7.65 (6H, d, J = 8 Hz), 7.44 (9H, m), 5.11 (6H, s), 3.96 (6H, s), 3.25 (2H, m), 2.42 (2H, t, J = 8 Hz), 1.98 (3H, s), and 1.10−1.40 (16H, m). HRMS (+ve ESI) calc for $C_{40}H_{50}NO_4$ 608.3734 m/z [M^+], found 608.3736 m/z. IR υ_{max} 2927, 2855, 1651, 1610, 1456, and 1267 cm^{-1}. UV λ_{max} (log ε) 387 (2.11), 278 (3.85) nm.

Cells and Cell Culture. Unless otherwise noted, tissue culture plasticware was from Becton Dickinson (Auckland, New Zealand), and cell culture reagents were from Invitrogen (Auckland, NZ). HL60 cells, originally from ATCC, were obtained from Dr. Graeme Findley (University of Auckland, NZ). Cells were grown in RPMI-1640 medium, supplemented with 5% fetal bovine serum (ICP Biotechnology, Auckland, NZ), GlutaMAX-1 (2 mM), penicillin (10 000 U/mL), streptomycin (10 000 μg/mL). The mitochondrial DNA-knockout cell line, HL60ρ^o, was derived from its parental cell line, HL60, by culturing in the presence of ethidium bromide (50 ng/mL)[29] for 6−8 weeks and lack of mitochondrial DNA verified by PCR and stable phenotype. Cells were cultured in RPMI-1640 medium, supplemented with 5% (v/v) heat-inactivated fetal bovine serum, 25 μg/mL penicillin, 25 μg/mL streptomycin, 50 μg/mL uridine, and 1 mM pyruvate. Both HL60 and HL60ρ^o were grown to densities of (0.5−0.8) × 10^6 cells/mL (exponential stage) at 37 °C in a humidified incubator maintained at 5% CO_2.

Biological Materials. 2-(4-Iodophenyl)-3-(4-nitrophenyl)-5-(2,4-disulfophenyl)-2*H*-tetrazolium monosodium salt (WST-1) and 1-methoxyphenazine methylsulfate (mPMS) were purchased from Dojindo Laboratories (Kumamoto, Japan). 2-(4,5-Dimethyl-2-thiazolyl)-3,5-diphenyl-2*H*-tetrazolium bromide (MTT) was purchased from Sigma-Aldrich (St Louis, USA).

tPMET Activity Measured by WST-1/*m*PMS Reduction. TPMET activity was measured as previously described.[30,31] Briefly, each compound dissolved in dimethyl sulfoxide (DMSO) was diluted 10-fold in HBSS from a starting concentration of 200 μM. 50 μL of each dilution was added to a 96-well, flat-bottomed microtiter plate (in triplicate). Exponentially growing cells were centrifuged at 2000 rpm for 2 min, washed and resuspended in HBSS buffer at a concentration of 2.0 × 10^6 cells/mL. 50 μL of cell suspension was added to a well containing 50 μL of compound, resulting in a final concentration of 1.0 × 10^6 cells/mL. Cells were incubated for 30 min at 37 °C in a humidified incubator maintained at 5% CO_2. Dye reduction was initiated by adding 10 μL of a 10× stock solution of WST-1/*m*PMS in Milli-Q water (final concentrations of 500 μM WST-1 and 20 μM *m*PMS). WST-1 reduction was measured in real time at 450 nm over 40 min in a FLUOstar OPTIMA plate reader (BMG Laboratories, Offenberg, Germany).

Cell Proliferation Measured by MTT Reduction. Each compound dissolved in dimethyl sulfoxide was diluted 3-fold in RPMI-1640 from a starting concentration of 50 μM. 50 μL of each dilution was added to a 96-well, flat-bottomed microtiter plate (in triplicate). Exponentially growing cells were centrifuged at 2000 rpm for 2 min, washed and resuspended in RPMI-1640 medium at a concentration of 0.4 × 10^6 cells/mL. 50 μL of cell suspension was added to a well containing 50 μL of compound, resulting in a final concentration of 0.2 × 10^6 cells/mL. Following 48 h incubation at 37 °C in a humidified incubator maintained at 5% CO_2, dye reduction was initiated by adding 10 μL of 5 mg/mL MTT to each well. After 2 h, 100 μL of lysing buffer was added and incubated overnight to allow formazan crystals to dissolve. Microtiter plates were then measured at A570 in a FLUOstar OPTIMA plate reader (BMG Laboratories, Offenberg, Germany).

Cell Cycle Arrest. Cells were seeded at 0.2 × 10^6 cells per mL in media (as described above). 30 μM of compound was added and cells incubated for 24 h at 37 °C in a humidified incubator maintained at 5% CO_2. After 24 h, cells were removed, washed in HBSS, and fixed with 70% cold ethanol. Fixed cells were spun at 3000 rpm for 5 min, resuspended in 1 mL of propidium iodide staining solution per million cells and incubated at 37 °C in a humidified incubator maintained at 5% CO_2 for 30 min. Cells were then analyzed for cell cycle arrest as a measure of apoptosis using flow cytometry (BD FACSort, Becton Dickson, San Jose, CA).

■ ASSOCIATED CONTENT

Supporting Information

NMR spectra, HPLC, and characterization checklist. This material is available free of charge via the Internet at http://pubs.acs.org.

■ AUTHOR INFORMATION

Corresponding Author

*Phone: +644 499 6914; fax: +644 499 6915; e-mail: mberridge@malaghan.org.nz.

Author Contributions

Manuscript equally written by Carole Grasso and Lesley Larsen.

Notes

The authors declare no competing financial interest.

■ ACKNOWLEDGMENTS

The authors would like to thank Genesis Oncology Trust for financial support for this work.

■ ABBREVIATIONS USED

APA, antiproliferative activity; DCM, dichloromethane; HRMS, high resolution mass spectrometry; PI, propidium iodide; TIA, tPMET inhibitory activity; tPMET, trans-plasma membrane electron transport

■ REFERENCES

(1) Herst, P. M.; Berridge, M. V. Plasma membrane electron transport: a new target for cancer drug development. *Curr. Mol. Med.* **2006**, *6*, 895−904.

(2) Lane, D. J.; Lawen, A. Transplasma membrane electron transport comes in two flavors. *Biofactors* **2008**, *34*, 191−200.

(3) Ly, J. D.; Lawen, A. Transplasma membrane electron transport: enzymes involved and biological function. *Redox Rep.* **2003**, *8*, 3−21.

(4) del Castillo-Olivares, A.; Nunez de Castro, I.; Medina, M. A. Dual role of plasma membrane electron transport systems in defense. *Crit. Rev. Biochem. Mol. Biol.* **2000**, *35*, 197−220.

(5) Medina, M. A.; del Castillo-Olivares, A.; Nunez de Castro, I. Multifunctional plasma membrane redox systems. *Bioessays* **1997**, *19*, 977−984.

(6) Fischer, H. Mechanisms and function of DUOX in epithelia of the lung. *Antioxid. Redox Signal* **2009**, *11*, 2453−2465.

(7) Lane, D. J.; Lawen, A. Ascorbate and plasma membrane electron transport–enzymes vs efflux. *Free Radical Biol. Med.* **2009**, *47*, 485−495.

(8) Houtkooper, R. H.; Canto, C.; Wanders, R. J.; Auwerx, J. The secret life of NAD+: an old metabolite controlling new metabolic signaling pathways. *Endocr. Rev.* **2010**, *31*, 194−223.
(9) Ying, W. NAD+/NADH and NADP+/NADPH in cellular functions and cell death: regulation and biological consequences. *Antioxid. Redox Signal* **2008**, *10*, 179−206.
(10) Baker, M. A.; Lane, D. J.; Ly, J. D.; De Pinto, V.; Lawen, A. VDAC1 is a transplasma membrane NADH-ferricyanide reductase. *J. Biol. Chem.* **2004**, *279*, 4811−4819.
(11) Ferreira, L. M. Cancer metabolism: the Warburg effect today. *Exp. Mol. Pathol.* **2010**, *89*, 372−380.
(12) Pavlides, S.; Whitaker-Menezes, D.; Castello-Cros, R.; Flomenberg, N.; Witkiewicz, A. K.; Frank, P. G.; Casimiro, M. C.; Wang, C.; Fortina, P.; Addya, S.; Pestell, R. G.; Martinez-Outschoorn, U. E.; Sotgia, F.; Lisanti, M. P. The reverse Warburg effect: aerobic glycolysis in cancer associated fibroblasts and the tumor stroma. *Cell Cycle* **2009**, *8*, 3984−4001.
(13) Lopez-Lazaro, M. The warburg effect: why and how do cancer cells activate glycolysis in the presence of oxygen? *Anticancer Agents Med. Chem.* **2008**, *8*, 305−312.
(14) Larm, J. A.; Vaillant, F.; Linnane, A. W.; Lawen, A. Up-regulation of the plasma membrane oxidoreductase as a prerequisite for the viability of human Namalwa rho 0 cells. *J. Biol. Chem.* **1994**, *269*, 30097−30100.
(15) Herst, P. M.; Tan, A. S.; Scarlett, D. J.; Berridge, M. V. Cell surface oxygen consumption by mitochondrial gene knockout cells. *Biochim. Biophys. Acta* **2004**, *1656*, 79−87.
(16) Scarlett, D. J.; Herst, P.; Tan, A.; Prata, C.; Berridge, M. Mitochondrial gene-knockout (rho0) cells: a versatile model for exploring the secrets of trans-plasma membrane electron transport. *Biofactors* **2004**, *20*, 199−206.
(17) Herst, P. M.; Berridge, M. V. Cell surface oxygen consumption: a major contributor to cellular oxygen consumption in glycolytic cancer cell lines. *Biochim. Biophys. Acta* **2007**, *1767*, 170−177.
(18) De Luca, T.; Morre, D. M.; Zhao, H.; Morre, D. J. NAD+/NADH and/or CoQ/CoQH2 ratios from plasma membrane electron transport may determine ceramide and sphingosine-1-phosphate levels accompanying G1 arrest and apoptosis. *Biofactors* **2005**, *25*, 43−60.
(19) Pelicano, H.; Xu, R. H.; Du, M.; Feng, L.; Sasaki, R.; Carew, J. S.; Hu, Y.; Ramdas, L.; Hu, L.; Keating, M. J.; Zhang, W.; Plunkett, W.; Huang, P. Mitochondrial respiration defects in cancer cells cause activation of Akt survival pathway through a redox-mediated mechanism. *J. Cell Biol.* **2006**, *175*, 913−923.
(20) Villalba, J. M.; Navas, P. Plasma membrane redox system in the control of stress-induced apoptosis. *Antioxid. Redox Signal* **2000**, *2*, 213−230.
(21) Prata, C.; Grasso, C.; Loizzo, S.; Sega, F. V.; Caliceti, C.; Zambonin, L.; Fiorentini, D.; Hakim, G.; Berridge, M. V.; Landi, L. Inhibition of trans-plasma membrane electron transport: a potential anti-leukemic strategy. *Leukemia Research* **2010**, *34*, 1630−1635.
(22) Herst, P. M.; Petersen, T.; Jerram, P.; Baty, J.; Berridge, M. V. The antiproliferative effects of phenoxodiol are associated with inhibition of plasma membrane electron transport in tumour cell lines and primary immune cells. *Biochem. Pharmacol.* **2007**, *74*, 1587−1595.
(23) Herst, P. M.; Davis, J. E.; Neeson, P.; Berridge, M. V.; Ritchie, D. S. The anti-cancer drug, phenoxodiol, kills primary myeloid and lymphoid leukemic blasts and rapidly proliferating T cells. *Haematologica* **2009**, *94*, 928−934.
(24) James, A. M.; Sharpley, M. S.; Manas, A. R.; Frerman, F. E.; Hirst, J.; Smith, R. A.; Murphy, M. P. Interaction of the mitochondria-targeted antioxidant MitoQ with phospholipid bilayers and ubiquinone oxidoreductases. *J. Biol. Chem.* **2007**, *282*, 14708−14718.
(25) King, M. P.; Attardi, G. Mitochondria-mediated transformation of human rho cells. *Methods Enzymol.* **1996**, *264*, 304.
(26) Morimoto, H. [Synthesis and biochemical actions of idebenone and related compounds. Ubiquinone and related compounds, XL]. *Naturwissenschaften* **1989**, *76*, 200−205.
(27) Asin-Cayuela, J.; Manas, A. R.; James, A. M.; Smith, R. A.; Murphy, M. P. Fine-tuning the hydrophobicity of a mitochondria-targeted antioxidant. *FEBS Lett.* **2004**, *571*, 9−16.
(28) Xie, M. W.; , T. S. A new protecting group for the synthesis of complex sulfonates. *Tetrahedron Lett.* **1996**, *37*, 4443−4446.
(29) Broadley, K.; Larsen, L.; Herst, P. M.; Smith, R. A.; Berridge, M. V.; McConnell, M. J. The novel phloroglucinol PMT7 kills glycolytic cancer cells by blocking autophagy and sensitizing to nutrient stress. *J. Cell Biochem.* **2011**, *112*, 1869−1879.
(30) Berridge, M. V.; Tan, A. S. Trans-plasma membrane electron transport: a cellular assay for NADH- and NADPH-oxidase based on extracellular, superoxide-mediated reduction for the sulfonated tetrazolium salt WST-1. *Protoplasma* **1998**, *205*, 74−82.
(31) Berridge, M. V.; Herst, P. M.; Tan, A. S. Tetrazolium dyes as tools in cell biology: new insights into their cellular reduction. *Biotechnol. Annu. Rev.* **2005**, *11*, 127−152.